

A NEW METHOD FOR HYSTERESIS MEASUREMENTS DEVELOPED FOR c_v -MEASUREMENTS AT THE CRITICAL POINT DURING THE D2-MISSION

J. Straub A. Haupt K. Nitsche
 L^ATTUM, Technische Universität München
 Arcisstr. 21, D-8000 München 2
 Germany

K. Kemmerle
 Kayser-Threde GmbH
 Wolfratshausenstr. 48, D-8000 München 70
 Germany

Abstract

The HPT (High Precision Thermostat) used during the D1-Mission is now modified for the D2-Mission. The new design provides the possibility to measure c_v in the critical region both during heating and cooling runs at an enlarged temperature range.

The unexpected results of the first μg -measurements of c_v performed during the D1-Mission can be explained by an asymmetrical mass distribution in the cell. There the sample was heated electrically, which provides highest accuracy in measuring caloric data, i.e. c_v , but only measurements from the two-phase region into the one-phase region are possible. Even at smallest temperature ramps (D1: +3.6 mK/h) the thermodynamic equilibrium cannot be reached, which is seen as the reason for the unexpected results of the D1-Mission. The new calorimeter is constructed in that way, that there the measurements start in the homogeneous density region above T_c , and the sample is cooled down into the two-phase region. In microgravity the density will remain homogeneous down to T_c and it is anticipated that the real value of c_v can be observed not being influenced by density stratification.

A fluid sample of SF_6 at the critical density is enclosed in a spherical cell, the energy transport between it and the surrounding shell, which can be heated and cooled continuously, takes place by radiation. By measuring the temperature difference between them as well as the temperature ramp of the sample cell itself, the heat capacity c_v is determined.

The paper describes the method and the design of the calorimeter, and the initial measurements demonstrate the functionality of the calorimeter concept. Not only the hysteresis effect between heating and cooling runs, caused by the different density stratification under earth conditions, but also a remarkably good agreement between the experimental results and the theoretical model behavior can be observed.

Keywords: Critical phenomena, isochoric specific heat, phase transition, radiation calorimeter, microgravity, D2-Mission

1 Introduction

Empirical equations of states for fluids are nowadays presented in terms of Helmholtz or Gibbs functions. These functions include the liquid and vapour regions, the advantage is that all thermodynamic equilibrium properties can be derived consistently. However, these functions are empirical and good experimental data are necessary to establish them. In particular, caloric data, especially the isochoric heat capacity c_v , is a property which is very sensitive even for theoretical considerations and modelling, since it is a measure of the energy average stored in the dynamic structure of molecules. Of special interest is that property at points of phase transition, because here the structure changes are of enormous interest for the understanding and theoretical modelling of the molecular structure in materials.

According to the definition of the specific heat capacity

$$c_v = c_v(T, \rho) = \left(\frac{\partial u}{\partial T} \right)_\rho \quad (1)$$

various methods have been developed to measure this property.

One of these is the stepwise heating of the cell to determine the cell capacity from the necessary energy and temperature increase. This method yields good results (Ref. [5, 10]), but can not be conducted during a time limited orbit mission due the long time constant for reaching temperature equilibration. Therefore, in many cases the scanning-ratio-method is used, where the sample cell is heated through the critical point and the surrounding shell follows with a constant temperature difference (in the most cases zero) between them. In both methods the sample cell is heated electrically, which provides the greatest accuracy for measurement of the heat input to the cell (Ref. [5, 10, 8]).

Measurements of c_v on earth, however, suffer from the existence of strong density stratifications due to the divergence of the isothermal compressibility χ_T , which, in many cases, can barely be resolved (Ref. [11]). c_v measurements somehow average over these local distributions and provide values that are not representative for a point of state, but rather for a range of fluid states.

Measurements with a high precision thermostat (HPT) therefore were conducted under reduced gravity (μg) during the Spacelab Mission (D1) in order to obtain a homogeneous density distribution. Resulting from these measurements, c_v revealed only a surprisingly gentle rise and smooth drop instead of the predicted peak at T_c . The result of subsequent extensive investigations with the unchanged flight hardware and numerical simulations (Ref. [10]) is that the long relaxation time for density equilibration after a perturbation, e.g. heating of the sample cell, is responsible for the surprising "hump" during these heating runs in orbit. A detailed explanation about these experiments is presented by Ref. [12, 10]. Numerical calculations of the D1 results demonstrate that such small temperature ramps performed by heating up the sample are required to guarantee density equilibration for the entire fluid. That would exceed the capabilities of the control equipment and also the experiment available time during a Spacelab Mission.

Cooling the sample from above T_c down to the two-phase region provides a much more convenient procedure for reaching the critical state in the entire volume, necessary for measuring the "real" behavior of c_v at the critical point. Thermostating the sample cell a few degrees above T_c provides a homogeneous density distribution which will remain during a moderate cooling down to T_c . Measuring the temperature inside the fluid as well as at the cell wall offers the possibility to verify the fast temperature equilibration ("critical speeding up"), which is predicted by several investigations e.g. Ref. [2, 9].

The hysteresis of c_v between cooling and heating runs for the same ramp value with the addition of recording the temperature distribution in the fluid provides information concerning the density distribution and density relaxation.

The heat transfer for cooling and heating of the sample is obtained by radiation. Cooling with Peltier elements was excluded because the stability for heat flux measurements is not sufficient. The existing concept of the HPT, e.g. mechanical structure and the technique of temperature measurement, resulted in the adoption of this solution, instead of using heat transfer by conduction. In principle, it can be described as a heat conduction calorimeter similar to that designed by Ref. [3] (see also Ref. [4]). At this place it should be mentioned, that cooling is the only method to reach the metastable liquid-vapour and liquid-solid region.

2 Experimental Apparatus

An assembly drawing of the HPT radiation calorimeter is shown in Fig. 1. For more detailed information about the HPT see Ref. [6, 7].

The mechanical structure consists of three cylindrical vessels (vessel 1-3), the spherical fluid sample 0 is contained in the spherical hollow vessel 1 called temperature reference.

Heating of vessel 1 can be done either passively by radiation, which occurs during the heating and cooling runs, or actively controlled by electrical heating, which is used to reduce the warm-up time until the constant ramp is

reached. The outer vessel 3 is heated only by the temperature of the chamber air, which is controlled by Peltier elements. Using copper for vessel 1 and AlMgSi1 for the outer shells provides fast equilibration of temperature gradients as well as suppressing of temperature disturbances originating from outside the thermostat due to high thermal conductivity and large heat capacity.

Uncontrolled heat exchange by convection is minimized by evacuation of the entire calorimeter up to 10^{-6} mbar. The vessels are fixed together with thin polyamide threads (Kevlar[®]) (4), which, together with thin electrical connectors (Flex Circuits, Minco Comp.) (5) reduce heat exchange by conduction between the vessels. Moreover, these flexible connections are necessary, because the vessels must be locked together to avoid damage by the strong vibrations during the launch and landing phases of the Space Shuttle. This is carried out by turning the locking knob (7), by which the bolt (6) is moved, which presses vessel 1 together with vessel 2 against vessel 3. After the launch, the lock is opened and the springs (not shown in Fig. 1), to which the end of the threads are tied, secure the vessels in a defined location (Fig. 1).

3 Measurement Method

Fig. 2 shows the heat transfer between the sample cell (Index 0) and the reference vessel (Index 1).

Thin Kevlar[®]-threads are used for holding the cell in place. They also minimize together with thin strings for the electrical connections the energy transport by heat conduction. The influence of these connections is determined by measuring the thermal resistance, as shown below.

Vessel 1 is heated and cooled with a linear temperature ramp between $T_c \pm 6$ K. The cell follows with a temperature difference proportional to the ramp rate \dot{T}_1 and the cell capacity $C_0(T)$. Measuring the temperatures T_0 and T_1 and introducing the parameters relevant for the heat transfer by radiation yields:

$$\dot{Q}_{\text{Rad},01} = \sigma_{01} \cdot A_0 \cdot (T_0^4 - T_1^4) \quad (2)$$

where

$$\sigma_{\text{Rad},01} = \frac{\sigma_s}{\frac{1}{\epsilon_0} + \frac{A_0}{A_1} \cdot \left(\frac{1}{\epsilon_1} - 1\right)} \quad (3)$$

with $\sigma_s = 5.67 \cdot 10^{-8}$ W/m² · K⁴ as Stefan-Boltzmann constant

ϵ_0, ϵ_1 emissivity of surfaces 0, 1

A_0, A_1 surface area of 0, 1

For the case with small temperature differences between T_0 and T_1 and a small variation of the absolute value of T_0 and T_1 , Eq. (2) can be linearized as:

$$\dot{Q}_{01} = \frac{1}{R_{\text{th}}} (T_0 - T_1) \quad (4)$$

Now, eq. 4 not only account for the heat transfer by radiation, but by heat conduction for constant conditions as well, which is justified by the negligible heat capacity of the strings.

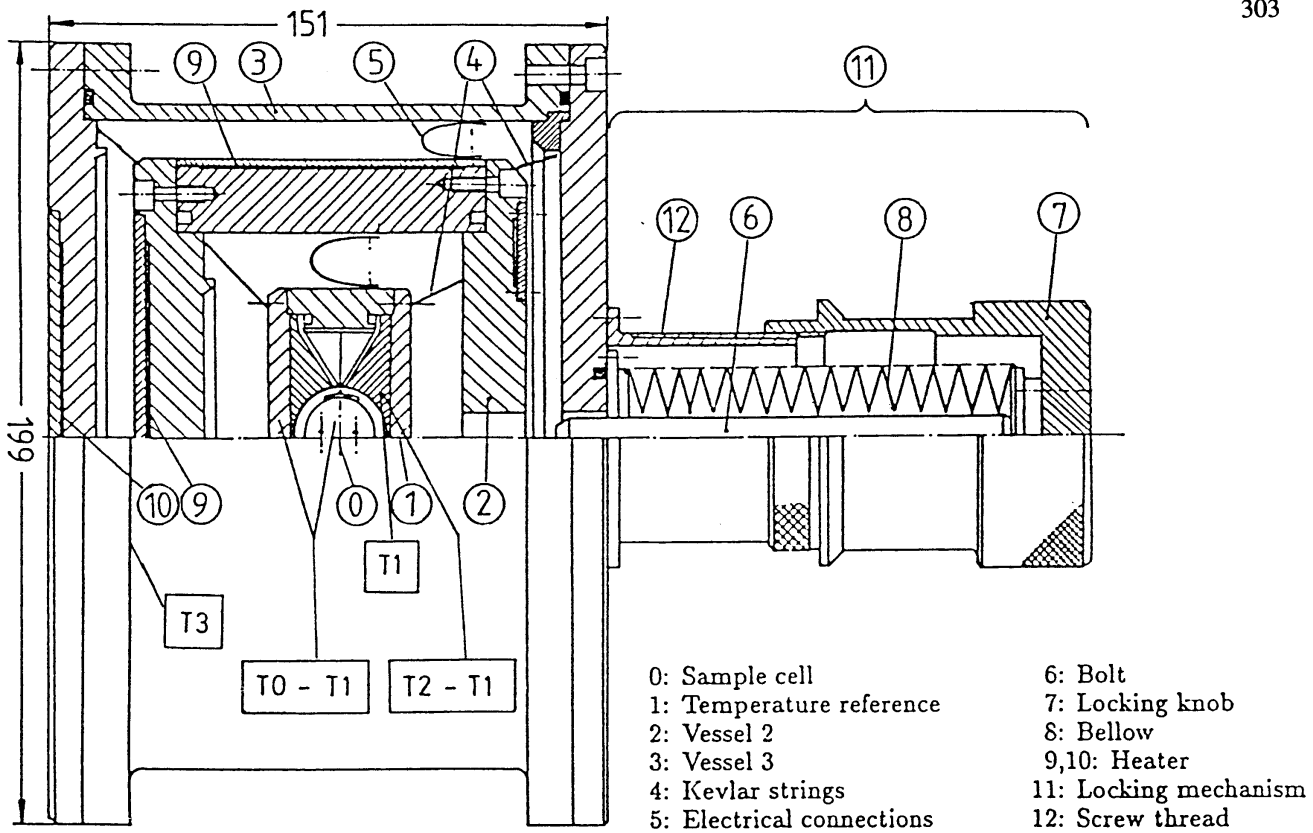


Figure 1: Functional structure of the HPT-calorimeter (unlocked) with a principal marking of the locations of temperature measurement(Ref.[6])

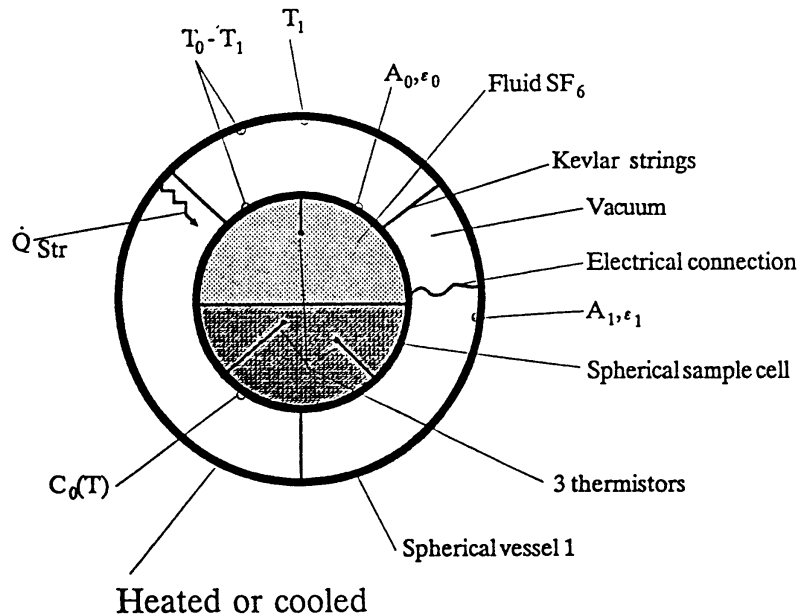


Figure 2: Heat transfer by radiation between the sample and the vessel 1

Employing eq. 4 requires an accurate determination of the thermal resistance R_{th} , which depends on the temperatures T_0 and T_1 , the geometry of the surface being used, the spectral characteristics and the conditions for the heat conduction through the connections. Assuming

R_{th} as a constant value gives a deviation of about 1 % in a temperature range of 1 K for the absolute value of the temperatures T_0 and T_1 and a range of the temperature difference $T_0 - T_1$ of 0.5 K, which is taken into account in the data evaluation.

R_{th} is determined by the steady electrical heating of the cell, with T_1 and T_0 constant, and measuring the electrical energy P_0 and the temperature difference $T_0 - T_1$:

$$P_0 = -P_{t,0} + \frac{1}{R_{th}}(T_0 - T_1) \quad (5)$$

$P_{t,0}$ is the energy dissipated by the electrical supply of the thermistor at the cell.

Finally, the capacity $C_0(T)$ of the sample during a cooling or heating run is given by an energy balance for vessel 0:

$$\dot{Q} = \frac{T_0 - T_1}{R_{th}} + P_{t,0} = C_0(T) \cdot \frac{dT_0}{dt} \quad (6)$$

where

$$C_0(T) = c_v(T) \cdot m_{SF_6} + C_c \quad (7)$$

with c_v specific heat

m_{SF_6} filling compound of SF_6

C_c capacity of the emptied cell.

The temperature rate $\frac{dT_0}{dt}$ is not measured directly, but is determined by differentiating the temperature difference $(T_0 - T_1)$ and the reference temperature T_1 :

$$\frac{dT_0}{dt} = \frac{d(T_0 - T_1)}{dt} + \frac{d(T_1)}{dt} \quad (8)$$

Providing a constant linear ramp for the reference vessel permits smoothing of the "step-like" development of T_1 caused by the digital measuring technique, which would cause peaks in the derivation $\frac{dT_1}{dt}$. This is achieved by heating vessel 2 and by controlling the temperature difference $(T_2 - T_1)$ during a given ramp to be constant, which is positive for heating and negative for cooling. Its absolute value defines the value of the temperature ramp of vessel 1. The slight variation of the heat transfer at different temperatures due to the nonlinear radiation law, however, causes a small bending of the curvature $T_1(t)$. This still yields a smooth curvature for $T_1(t)$ and a smooth derivative $\dot{T}_1(t)$.

The large heat capacity C_1 and high conductivity compensate for the small disturbances of the heat transfer caused by the digital controlling of the electrical power for vessel 2. The ratio of about 100:1 of the heat capacities C_1 and C_0 minimizes a deviation of $\frac{dT_1}{dt}$ caused by the diverging value of $C_0(T)$ at T_c .

Vessel 3 is heated or cooled by the chamber air on a similar ramp, which provides constant heat transfer by radiation between these shells. During the cooling runs the energy of the inner shells is transported out of the calorimeter by cooling the chamber air with Peltier elements, which in turn produces negative gradients between all vessels.

4 Temperature Measurement

Table 1 presents the vital data concerning the measurement of the most important experiment temperatures.

The measurement of the absolute temperatures T_1 and T_3 and of the temperature differences $T_2 - T_1$ and $T_0 -$

T_1 is made by thermistors in Wheatstone bridges and subsequent amplification with Lock-in-amplifiers (LIA). The temperature difference $T_0 - T_1$ is measured using only one thermistor at a time in order to minimize the power dissipated to the fluid. Each of the four matched sensors is active for a total of two minutes, but there is also the possibility of recording for a longer time period.

In addition, two platinum resistance thermometers Pt25 (Rosemount, 162D), with a stability better than 0.010 K/a are used to measure the absolute value of T_1 . As a result, the influence of the drift rate of the thermistors, already reduced by artificial aging, can be compensated by periodic calibration. In case of the possible damage of these shock sensitive sensors, extrapolating the calibration curvature for each thermistor provides an opportunity for correcting the temperature data obtained during the mission.

In order to obtain the required larger measurement range with the high accuracy as used in the earlier thermostat concept, the existing measuring techniques were modified: if the bridge voltage exceeds the range of the LIA because of a growing temperature difference at the thermistors, a constant resistance, controlled by software, is switched on to the side of the bridge with the lower resistance, changing the measuring range.

During the rise time of the LIA after such a change as well as a change of the sensor measuring $T_0 - T_1$, the old value is retained to avoid a deviation of the control. An accurate correction is conducted in the evaluation of the data recorded with an external computer.

5 Sample Cell

Instead of the coin-shaped cell of the D1 thermostat, with a hydrostatic height of 1 mm, a spherical cell is now used (Fig. 3). Experiments conducted under μg on a KC-135 flight result in a predicted defined phase distribution for the spherical cell (inner diameter of 2 cm): The fluid completely wets the inner surface, which forms a concentric gas bubble. This distribution provides a maximum length for mass diffusion of about 4mm, which can be taken into account for the evaluation of c_v better than the uncertain mass distribution in the D1 cell (for more information see Ref. [10]).

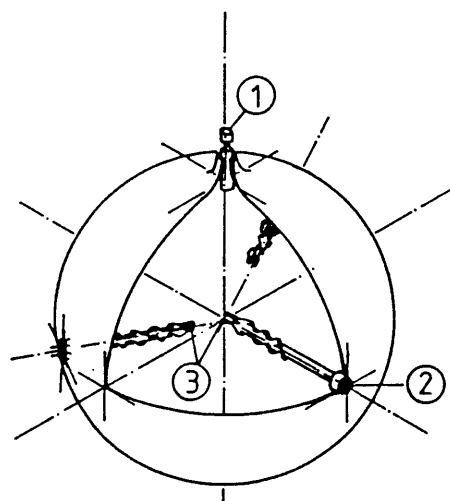
This form also allows the measurement of the temperature distribution inside the fluid, which is obtained by three thermistors located at different distances from the wall.

The sphere is produced by electrolytical coating of an aluminum core with four different layers, followed by dissolving the core with acid. The inner layer is made of gold, to avoid chemical reactions with the test fluid. The stress carrying layer third consists of copper, due its strength as well as its high thermal conductivity, which provides good heat transfer from the surface to the fluid. The second layer of silver serves as a shield for the diffusion of gold into the copper. The outer layer protects the copper from corrosion.

TABLE 1

| Measurable variable | Used sensor | Meas. range accuracy | Physical resolution $\hat{=} 1\text{LSB}$ |
|------------------------------------|---|--|---|
| Absolute Temperature T_1 | Thermistor YSI 44908 | $T_c \pm 6\text{ K } \pm 10\text{ mK}$ | $0.18 \div 0.29\text{ mK}$ |
| | Pt 25 162 D (Rosemont) | $T_c \pm 6\text{ K } > \pm 10\text{ mK}$ | 2.93 mK |
| | Pt 25 162 D (Rosemont) | $T_c \pm 0.5\text{ K } > \pm 10\text{ mK}$ | 0.24 mK |
| Absolute Temperature T_3 | Thermistor YSI 44908 | $10 - 60^\circ\text{C } \pm 100\text{ mK}$ | 24 mK |
| Temperature Difference $T_0 - T_1$ | Thermistor GB42JM86 (Fenwal Electronic) | $T_c \pm 2\text{ K } \pm 0.2\text{ mK}$ | $0.011 \div 0.017\text{ mK}$ |
| Temperature Difference $T_2 - T_1$ | Thermistor YSI 44908 | $T_c \pm 6\text{ K } \pm 2\text{ mK}$ | $0.27 \div 0.45\text{ mK}$ |

Data of experiment temperatures



1. Filling capillary
2. Bushing
3. Matched thermistors

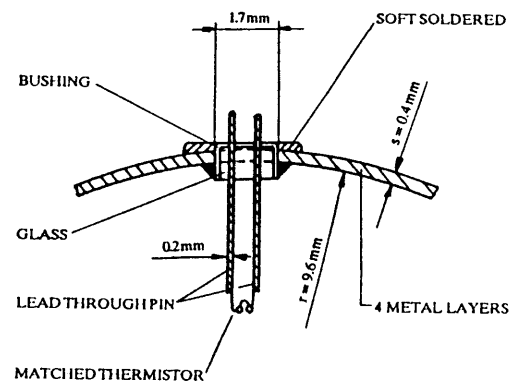


Figure 3: Sphere-shaped cell used in the D2-HPT

Figure 4: Detailed view of a bushing

With production processes such as deep-draw or lathe operations, such a uniform layer thickness and homogeneous crystal structure could not be produced.

The electrical bonding of the thermistors inside the cell (Fig. 4) is made by small bushings (Schott Company), which are soft soldered in the cell wall. Using SF₆ ($p_c = 37,6$ bar), a total wall thickness of about 0.10 mm is sufficient for operation. The layer size of the flight wall, however, amounts to 0.4 mm due to the limited creep-strength of the soft solder and a desired cell life-time of about 4 years.

Finally, the sphere provides a symmetrical energy supply to the cell, which avoids azimuthal temperature gradients.

The leak rate of different cells filled with SF₆ was determined by a long-time measurement and an analysis with a mass spectrometer, and is below the detection limit.

The critical density of the specimen (SF₆ of 99.993 % liquid purity, Matheson Gas Products) was determined by a weighing procedure in comparison with a known reference volume. Taking thermal and pressure expansion of the cell into account, the overall error ± 0.5 % was calculated to be less than the error of the critical density $\rho_c = 0.737$ g/cm³ found in literature (Balzarini, 1974, and private communication with Michels, from van der Waals Laboratory). Several cycles of evacuating (24 h) and flushing the cell guarantees high specimen purity.

6 Results, Discussion

To demonstrate the functionality of the calorimeter, the determination of the total cell capacity C_0 are presented here for a heating and a cooling run with the same value of the temperature ramp.

The data, recorded at 1 sec intervals (highest data rate: one measurement every 0.6 sec), was corrected for the changes in the temperature ranges and the divergence of the thermistors. An exact evaluation of the data to yield specific isochoric heat c_v is only possible after the emptying of the sample cell and the determination of the heat capacity of the sphere itself (see Eq. (7)).

Fig. 5 shows the hysteresis in the behavior of C_0 of equal heating and cooling runs, in general the same behaviour of C_0 is obtained for runs with other temperature ramps. These initial 1-g data are compared with the behaviour of c_v predicted by the theoretical Power Law.

As expected, the heating runs based on the delay in the density conditions in the relatively fast ramps show a flattened curvature of c_v in the critical region. The comparison of different heating runs demonstrates, that faster ramps cause a stronger deviation towards the model curve because of a greater difference between the existing density distribution towards the equilibrium distribution.

A completely different condition is to be seen during the cooling runs. A clearly defined peak in c_v is visible here in all runs. The density field, which was homogenized above T_c , is not influenced by the diverging compressibility due to the long density relaxation time. So nearly the entire volume goes beyond the critical state in a short time period, which results in this pronounced peak in c_v .

These results are in full agreement with current investigations on measuring of c_v conducted by Ref. [5, 10].

A view of the behavior of c_v at cooling in the two-phase region shows, that c_v first decreases more than the model curve, and then crosses it and finally after a small "hump" runs into the model curve. This could be explained either by a delay in the equilibration of the density field, which means a delayed release of the energy of the density shift, or as a result of the dynamic processes in the sample, which occurs a few mK below T_c .

The temperature difference $T_0 - T_1$ (Fig. 6) here oscillates a few minutes during all cooling runs after crossing T_c . This effect depends clearly on a oscillation of the temperature T_0 itself, because T_1 decreases with a linear ramp. This observation could be a result of alternately subcooling and subsequent condensation of a part of the vapor with an abrupt release of condensation energy. Similar observations were made during our recently conducted experiments with the Critical Point facility (CPF) during the IML-1 Mission:

The phase separation in the flat cylindrical cell happened in the expected way by condensation of the fluid at the cooler wall, which formed a ring-shaped fluid phase and a central gas bubble. During the incessant cooling of the sample into the two-phase region local condensation in the gaseous phase and also local evaporation in the fluid phase took place. The evaluation of all these recordings should assist in understanding these phenomena.

7 Conclusions

A radiation heat calorimeter for the study of the hysteresis of c_v between heating and cooling ramps was constructed. The heat transfer between the sample cell and the surrounding shell by radiation permits determination of the specific isochoric heat c_v in a domain of ± 6 K from the critical point, as well as during heating and cooling runs. In addition, the temperature field of the sample is measured by three thermistors. The initial results under earth conditions yield the expected hysteresis during the courses between heating and cooling runs.

The cooling runs, despite the fact of the large hydrostatic height of the sphere-shaped sample cell and the comparably fast temperature ramp rates, provided a clearly defined peak of c_v at the critical point, which almost matches the theoretical model behavior. The concept, together with a fast data rate and a highly accurate temperature measurement system provides the opportunity for recording the fast processes which occur during cool down to the critical point, and the not yet explained effects which take place during the phase transition in the two-phase region.

The current area of concentration is the development of an adequate experiment timeline for the investigations of c_v and its hysteresis planned for the D2-Mission, with special consideration for a manned space flight. This also includes further evaluation of experimental runs with the D2-HPT and corresponding experiments with other facilities providing optical recording.

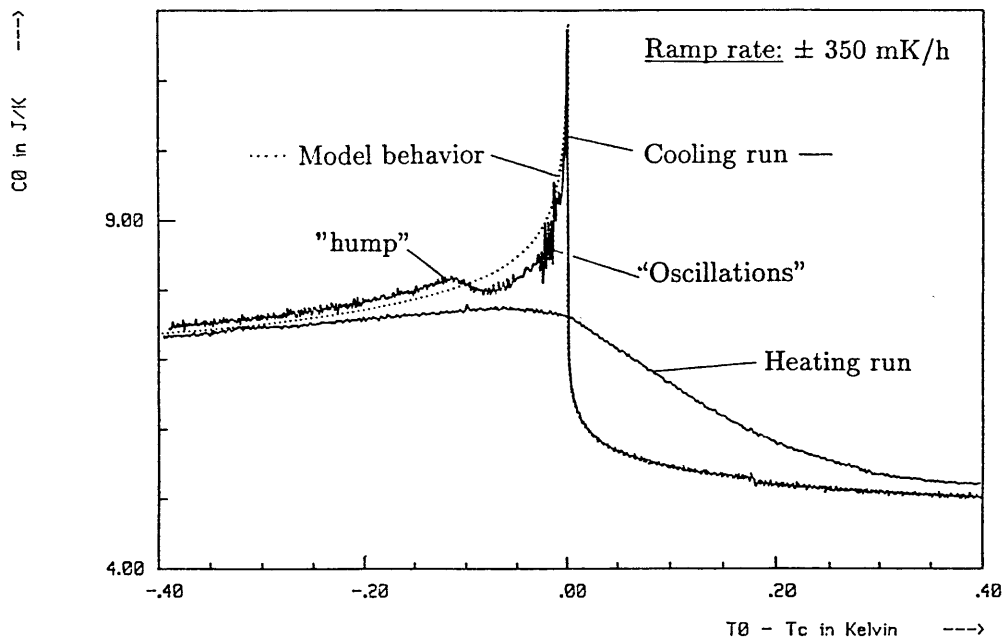


Figure 4: Hysteresis of the total cell capacity C_0 between a heating and a cooling run with an equal ramp \dot{T} under 1g conditions.

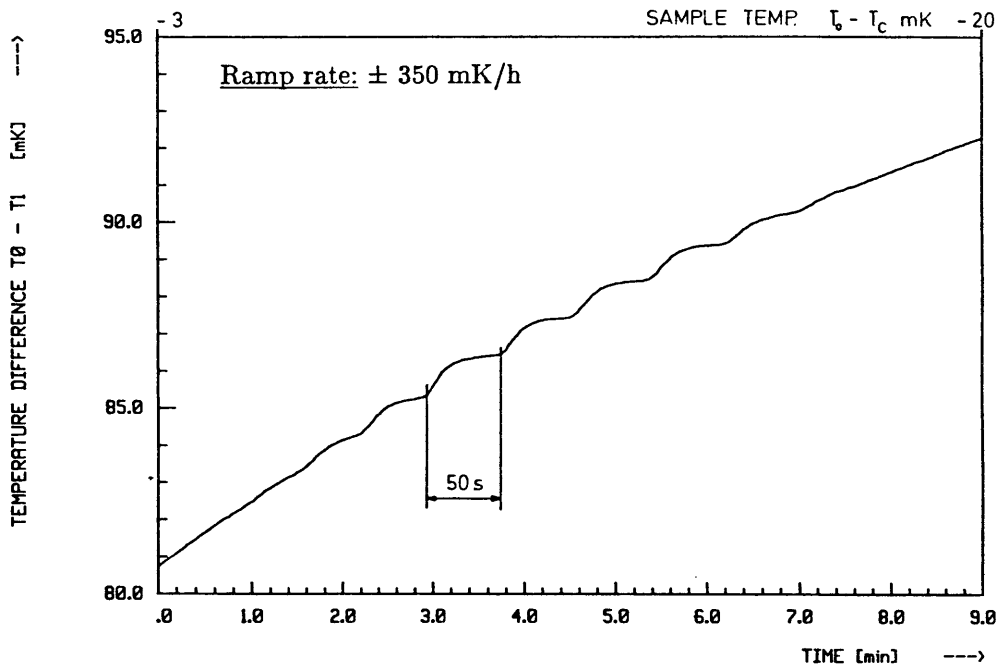


Figure 5: Oscillations of the temperature difference $T_0 - T_1$ during cooling into the two-phase region

Acknowledgements

The authors are grateful to the Deutsches Bundesministerium für Forschung und Technologie (BMFT) for financial support of this research. They also wish to express their appreciation to DARA and DLR for the project managing.

References

- [1] Balzarini, D.; Palfy, P.: *Density Dependence of LL -Coefficient for SF_6* , Can. J. Phys. **52**, p 2007, 1974
- [2] Boukari, H.; Shaumeyer, J.N.; Briggs, M.E.; Gammon, R.W.: *Critical speeding up in pure fluids*, Phys. Rev. A **41**, pp 2260–2263, 1990
- [3] Calvet, E.: *Recent Progress in Microcalorimetry*, In: H.A. Skinner (Ed.), Exp. Thermochemistry, Vol. II Interscience Publishers, New York, 1962
- [4] Calvet, E.; Prat, H.: *Recent Progress in Microcalorimetry*, Pergamon Press, 1963
- [5] Edwards, T.J.: *Specific heat measurements near the critical point of carbon dioxide*, Thesis, University of Western Australia, 1984
- [6] Kayser-Threde.: *Spacelab-Mission D2, Nutzlastelement MEDEA, Spezifikation für die Mehrzweckanlage Hochpräzisions-Thermostat (HPT) mit dem Experiment HYDRA, D2-MD-SP-030-KT, Issue 1, Revision A, August 1989, Deutsche Gesellschaft für Luft- und Raumfahrt DFVLR, Köln, 1989*
- [7] Kemmerle, K.: *The High Precision Thermostat HPT-HYDRA*, t.b.p., Kayser-Threde GmbH, München, 1992
- [8] Lange, R.; Straub, J.: *Die isochore Wärmekapazität fluider Stoffe im kritischen Gebiet — Voruntersuchungen zu einem SPACELAB-Experiment*, Forschungsbericht W 84-034 Bundesministerium für Forschung und Technologie, 1984
- [9] Nitsche, K.; Straub, J.; Lange, R.: *Ergebnisse des TEXUS-8-Experiments Phasenumwandlung*, Forschungsbericht Luft- und Raumfahrt, BMFT, 1984
- [10] Nitsche, K.: *Die isochore Wärmekapazität im kritischen Gebiet von Schwefelhexafluorid unter Erdschwere und reduzierter Schwere bei verzögertem Dichtenausgleich*, Thesis, Technical University Munich, 1990
- [11] Straub, J.: *Dichtemessungen am kritischen Punkt mit einer optischen Methode bei reinen Stoffen und Gemischen*, Thesis, Technical University Munich, 1965
- [12] Straub, J.: *Isochoric Heat Capacity c_v at the Critical Point of SF_6 under Micro- and Earth Gravity, Experimental Results of the Spacelab Mission D1*, paper presented at the 11th Symposium on Thermophysical Properties, t.b.p., 1991